Numerical simulation of magnons

Sondre Duna Lundemo†
Department of Physics, Norwegian University of Science and Technology, Trondheim
Norway
TFY4235 - Computational physics
(*Last updated on February 23, 2021*)

†sondre@duna.no

Contents

PART
I

Introduction & Background

1 Theoretical background

Hamiltonian

$$H = -\frac{1}{2}\sum_{j,k}^{N} J_{jk}\mathbf{S}_j \cdot \mathbf{S}_k - d_z \sum_{j=1}^{N}(S_{j,z})^2 - \mu \sum_{j=1}^{N} \mathbf{B}_j \cdot \mathbf{S}_j \tag{1}$$

Landau-Lifshitz-Gilbert equation

$$\partial_t \mathbf{S}_j = \frac{-\gamma}{\mu(1+\alpha^2)} \left[\mathbf{S}_j \times \mathbf{H}_j + \alpha \mathbf{S}_j \times (\mathbf{S}_j + \mathbf{H}_j)\right] \tag{2}$$

where

$$\mathbf{H}_j = -\frac{\partial H}{\partial \mathbf{S}_j} + \boldsymbol{\xi}_j \tag{3}$$

2 Code overview

PART II

Results and discussion

3 Single spin

3.1 Precession of spin in uniform magnetic field

We simulate the time evolution of a single spin $\mathbf{S}$ in the presence of a uniform magnetic field $\mathbf{B} = (0, 0, B_0)^T$ in the $\mathbf{e}_z$-direction. The components of the spin at equidistant time steps during one period are shown in figure 1. As expected, we see that the spin precesses around the effective field $\mathbf{H}$, which in this case is given by

$$\mathbf{H} = -\frac{\partial H}{\partial \mathbf{S}} = \frac{\partial}{\partial \mathbf{S}} (\mu \mathbf{B} \cdot \mathbf{S}) = \mu \mathbf{B},$$

in the absence of damping and anisotropy.

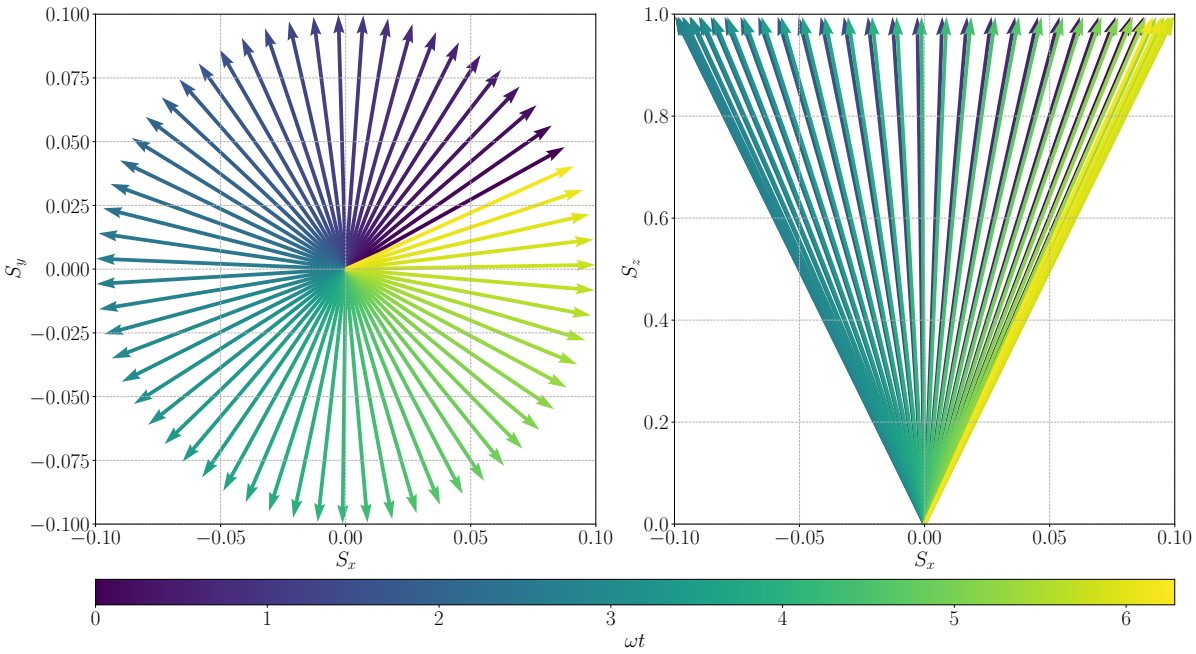

Figure 1: The figure shows the x and y component of the spin during one period in a uniform magnetic field without further interactions.

In this particular case, we can easily find an analytical solution to compare with. The LLG-equation reads

$$\partial_t \mathbf{S} = -\frac{\gamma}{\mu} \mathbf{S} \times \mathbf{B}.$$

As $\mathbf{B} = (0, 0, B_0)^T$,

$$\mathbf{S} \times \mathbf{B} = (S_y \mathbf{e}_x - S_x \mathbf{e}_y) B_0.$$

Thus, we have two equations

$$\begin{cases} \partial_t S_x = -\gamma B_0 S_y \\ \partial_t S_y = \gamma B_0 S_x. \end{cases} \tag{4}$$

which are easily solved by differentiating both with respect to t, and then substituting the first order derivatives on the right hand side by the corresponding expressions in 4.

$$\begin{cases} \partial_t^2 S_x = -\gamma B_0 \partial_t S_y \\ \partial_t^2 S_y = \gamma B_0 \partial_t S_x. \end{cases} \tag{5}$$

This yields the two equations

$$\ddot{S}_x = -\left(\gamma B_0\right)^2 S_x \quad ; \quad \ddot{S}_y = -\left(\gamma B_0\right)^2 S_y, \tag{6}$$

which have solutions

$$S_x(t) = S_x(0)\cos\left(\omega t\right) - S_y(0)\sin\left(\omega t\right) \tag{7}$$
$$S_y(t) = S_y(0)\cos\left(\omega t\right) + S_x(0)\sin\left(\omega t\right), \tag{8}$$

with the frequency $\omega = \gamma B_0$. When comparing the exact solution with the numerical estimate obtained through integrating the LLG-equation with Heun's method, the trajectories of S_x and S_y are as shown in figure 2.

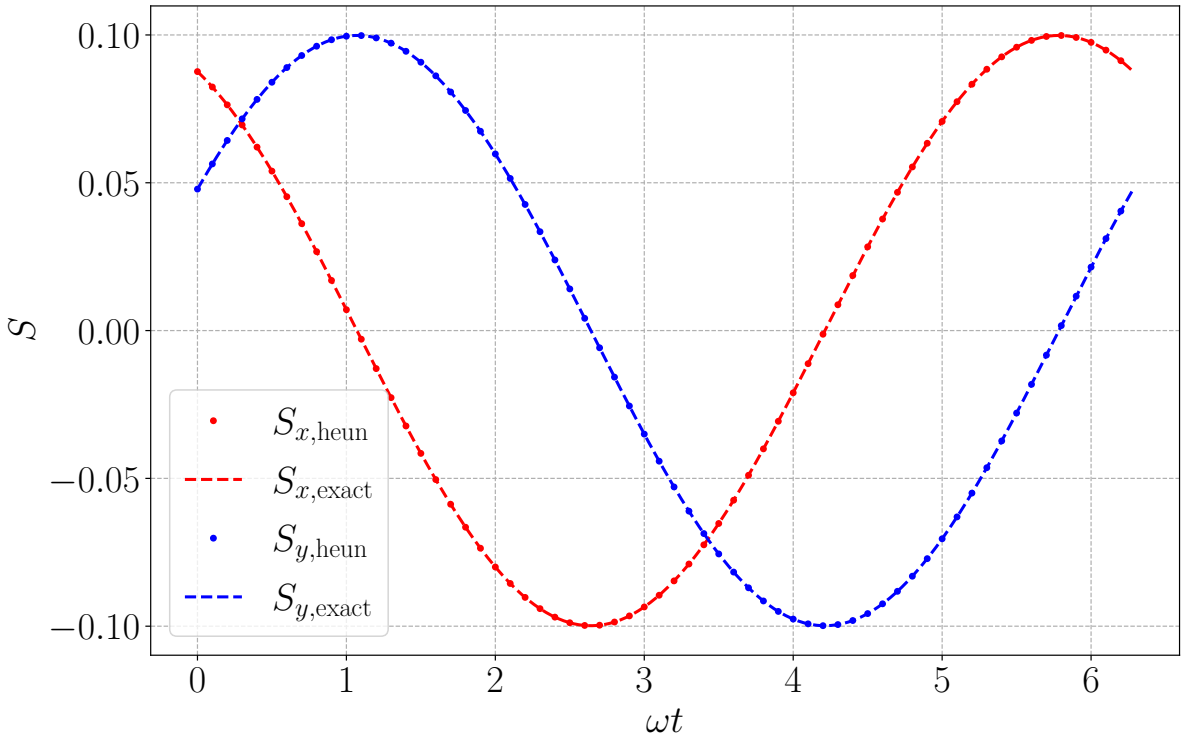

Figure 2: The plot shows the exact solution given in (7) and (8) compared with the numerical solution sampled at every tenth step to be able to distinguish the paths.

It is perhaps more enlightening to consider the pointwise difference of the exact and numerical solution. This is shown in figure 3. The figure shows that the deviations locally oscillate, but globally, of course, the absolute deviation increases.

References

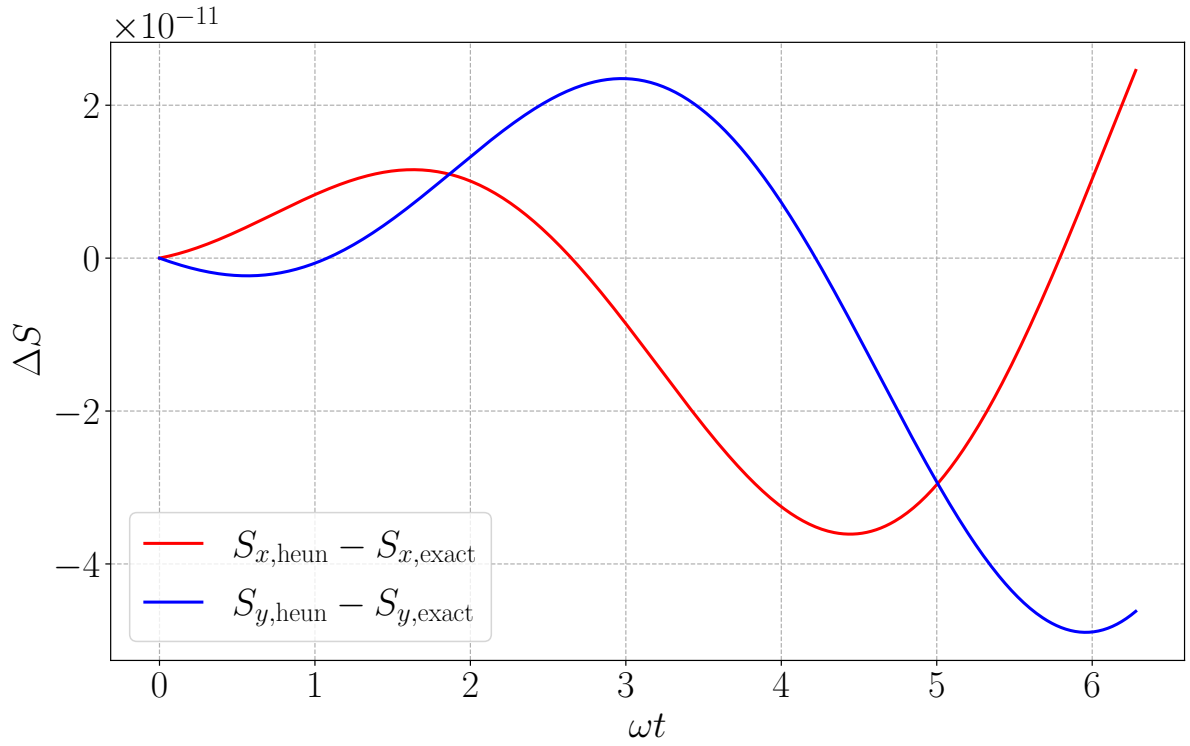

Figure 3: The plot shows the difference between the exact solutions given in (7) and (8), and the numerical solutions over one period.